Journal of Applied Polymer Science

Influence of the Interfacial Adhesion on the Stringiness of Crosslinked Polyacrylic Pressure-Sensitive Adhesives

Keiko Ito,[1] Kohei Shitajima,[1] Nozomi Karyu,[1] Syuji Fujii,[1] Yoshinobu Nakamura,[1] Yoshiaki Urahama[2]

[1]Department of Applied Chemistry, Osaka Institute of Technology, 5-16-1 Ohmiya, Asahi-ku, Osaka 535-8585, Japan

[2]Graduate School of Engineering, University of Hyogo, 2167 Shosha, Himeji, Hyogo 671-2201, Japan

Correspondence to: Y. Nakamura (E-mail: nakamura@chem.oit.ac.jp)

ABSTRACT: The stringiness of crosslinked polyacrylic pressure-sensitive adhesives (PSA) was observed during 90° peeling under a constant peel rate with various adherends in order to clarify the influence of interfacial adhesion on the stringiness behavior. The crosslinked random copolymer of butyl acrylate with 5 wt % acrylic acid was used as a representative PSA. Poly(methyl methacrylate) (PMMA), polycarbonate (PC), poly(vinyl chloride) (PVC), fused quartz plates and some surface-modified poly(ethylene terephthalate) films were used as adherends. The films were pasted on a glass plate using a cyanoacrylate adhesive. The 180° peel strength was higher in the order of PVC >> PMMA ≈ PC > other adherends. All observed stringiness was sawtooth-shaped, but the stringiness width and length were longer in the same order. The number of sub-branches formed at the tips of the strings was much more for the PVC, PMMA and PC adherends. Frames formed at the front end of the strings in the case of PVC adherend. Sufficient interfacial adhesion generates large internal deformation of the PSA layer. Internal deformation occurred preferentially over peeling as a result of front frame formation. The string length and the peel load required for the constant peel rate have good correlation with the peel strength. The estimation of generated inner stress in the fibrils of the strings was possible by analysis using the string length for various adherends and the stress–strain curve of pure PSA. © 2014 Wiley Periodicals, Inc. J. Appl. Polym. Sci. **2014**, *131*, 40869.

KEYWORDS: adhesives; copolymers; surfaces and interfaces; viscosity and viscoelasticity

Received 12 January 2014; accepted 14 April 2014

DOI: 10.1002/app.40869

INTRODUCTION

The stringiness of pressure-sensitive adhesives (PSA) is observed at the tip part of peeling during peel testing. Some researchers have investigated this stringiness phenomenon.[1–9] Kaelble[1] clarified that the stringiness disperses the applied stress concentrated at the tip part of peeling and increases the peel strength. Urahama[2] reported two types of string shapes that are dependent on the backing materials of the PSA tape, i.e., sawtooth- and honeycomb-shaped. Urahama[2] clarified that the shape of the strings is strongly dependent on the interfacial adhesion, the viscoelastic properties of the PSA and the peel rate. However, the influence of the cohesive strength of PSA on the shape of the strings has not yet been investigated using a PSA with continuous variation of the cohesive strength.

In our previous report,[10] the influence of the cohesive strength of PSA on the shape of the stringiness was investigated. The random copolymer of butyl acrylate (BA) with 5 wt % acrylic acid (AA) [P(BA-AA)] crosslinked by *N*,*N*,*N*′,*N*′-tetraglycidyl-*m*-xylenediamine was used as a representative PSA. The crosslinker content was in the range of 0–0.016 chemical equivalents (Eq.). The cohesive strength of PSA changes depending on the crosslinking degree. Fused quartz plate was used as an adherend. As a result, all observed stringiness upon peeling was sawtooth-shaped, but it could be classified into three types dependent on the degree of crosslinking. The typical sawtooth-shaped stringiness with interfacial failure was observed at a relatively higher crosslinker content ranging from 0.008 to 0.016 Eq., where the PSA has high cohesive strength and low interfacial adhesion. Frames formed at the front end of the strings at contents ranging from 0.002 to 0.004 Eq. Sufficient interfacial adhesion and deformability generate large internal deformation of the PSA layer. Internal deformation occurred preferentially over peeling as a result of front frame formation. The mode of peeling was changed from cohesive failure to interfacial failure in this range of crosslinker content. The sawtooth-shape with cohesive failure was observed at the lower content ranging from 0 to 0.001 Eq. The PSA has high interfacial adhesion and low cohesive strength, and thus exhibits cohesive failure. The PSA after peeling remained in the shape of belts. It was found that the shape of the strings was strongly dependent on the balance between the interfacial adhesion and the

cohesive strength of PSA. When the sawtooth-shaped stringiness with frame formed, the peeling rate was lowest. This means the peel strength should be the maximum with this shape of stringiness.

In this paper, the influence of interfacial adhesion on the stringiness was investigated using the crosslinked P(BA-AA) PSA with a constant crosslinker content and various adherends. Some polymer plates and poly(ethylene terephthalate) (PET) films with various surface modifications were also used as adherends. The PET films were pasted on the slide glass plate using a cyanoacrylate adhesive. The relationship between the interfacial adhesion and the shape and the length of strings were discussed. The estimation of generated inner stress in the strings was made using the string length and the stress–strain curve of pure PSA.

EXPERIMENTAL

Materials

P(BA-AA) with 5 wt % AA [weight average molecular weight (M_w) of 500,000, polydispersity of 4.9, 40 wt % ethyl acetate solution, synthesized by Toagosei, Tokyo, Japan] was used as a base polymer. *N,N,N',N'*-Tetraglycidyl-*m*-xylenediamine (Tetrad-X, Mitsubishi Gas Chemical Company, Tokyo, Japan) was used as a crosslinker. Reagent grade ethyl acetate was used as a solvent.

Plates used as adherends: poly(methyl methacrylate) (PMMA, 2 mm thickness, Paltec Test Panels, Kanagawa, Japan), polycarbonate (PC, 2 mm thickness, Paltec Test Panels, Kanagawa, Japan), poly(vinyl chloride) (PVC, 2 mm thickness, Mitsubishi Plastics, Tokyo, Japan), stainless steel (SS, 1.5 mm thickness, SUS304-BA, Nihon Tact, Kanagawa, Japan) and fused quartz (Quartz, 2 mm thickness, commercial item). The polymer plates were made by molding. Some films were also used as adherends: biaxial oriented polypropylene (OPP, 40 μm thickness, Toyobo, Osaka, Japan), PET without treatment (PET, 38 μm thickness, Toray Industries, Tokyo, Japan), flat-treated PET (F-PET, 50 μm thickness, Cosmoshine A4100, Toyobo, Osaka, Japan), high adhesion-treated PET (HA-PET, 100 μm thickness, Cosmoshine A4300, Toyobo, Osaka, Japan), hard coated PET (HC-PET, 265 μm thickness, Nakai Industrial, Kyoto, Japan), and silicone-coated PET (Si-PET, 38 μm thickness, donated by Lintec, Tokyo, Japan). These films were pasted on a slide glass plate (1 mm thickness, S7213, Matsunami Glass Ind., Osaka, Japan) using a cyanoacrylate adhesive.

Sample Preparation

A 1 wt % ethyl acetate solution of the crosslinker was prepared and a predetermined amount of 0.016 Eq. was added to the P(BA-AA) solution. Ethyl acetate was added to prepare a solution at a constant concentration of 30 wt % and the mixture was stirred. The solutions were coated on PET sheets (38 μm thick) using an applicator (Baker type, SA-201, Tester Sangyo, Saitama, Japan). The coated films were heated at 120°C for 3 min to evaporate the ethyl acetate. Paper coated with a silicon release agent was then attached to the surface of the coated PSA film and heated at 60°C for 20 h to accelerate the crosslinking reaction. The thickness of the resulting PSA layer was measured using a thickness indicator (Dial thickness gauge H-MT, Ozaki, Tokyo, Japan) and was determined to be approximately 50 μm.

The PSA solution was also cast on a silicone release agent-coated PET sheet to prepare specimens for tensile tests.

Tensile Properties

The square (50 × 50 mm) ca. 50 μm thick PSA films were rolled up to prepare cylindrical samples. The cylindrical samples were then tested using a tensile testing machine (AG-5KNIS, Shimadzu, Kyoto, Japan) with a chuck distance of 10 mm and a tensile rate of 100 mm·min^{-1} to obtain stress–strain curves in the same way as the previous reports.[11,12]

Peel Strength

The prepared PSA tapes were cut into 25 mm wide strips and a strip was then placed onto the adherend plate (50 × 100 × 2 mm). The strip of PSA tape was pressed on the adherend using a 2 kg iron roller (90 mm diameter, rubber-coated surface) to develop good contact between the PSA and adherend. Test specimens were subjected to five press cycles, where one press cycle involved the iron roller being moved backward and forward. The peel strength was measured 20–30 min after specimen preparation.

The 180° peel strength was measured at a peel rate of 300 mm·min^{-1} at 23–25°C using a tensile testing machine (AG-5KNIS, Shimadzu, Kyoto, Japan) in accordance with JIS Z 0237 (Japanese Industrial Standards) and PSTC 101 in the same way as in the previous study.[13]

Observation of Stringiness

The PSA tapes of 25 mm width were placed onto an adherend plate and pressed using a 2 kg iron roller. This sample preparation method is the same as that for the peel strength test. The stringiness was observed 20–30 min after specimen preparation.

The stringiness during 90° peeling was observed using the apparatus for stringiness observation shown in our previous report.[10] A weight was hung at the tip of the adhered PSA tape. Weights of 20 or 200 g are equivalent to an applied force of about 0.2 or 2 N, respectively. The desired weights were connected in series and loaded. The stringiness was recorded using a digital microscope (TG3000PC, Edenki, Kyoto, Japan) for upper and side views when the peeling was in a stationary state. The peel rate was calculated from the time taken for the stringiness to progress a constant distance. The observed upper (a) and side (b) views of stringiness are shown in Figure 1. The length of the strings was clearly observed from the upper view, which is referred to as the deformation width. The stringiness width and length were measured from the side view. The sub-branches were observed at the tip of the strings for some adherend as shown in Figure 1. The angle of the sub-branches was measured as shown in Figure 2 and shown by the average value of the measured angle.

The surface of plate adherend as-received was covered with a protection film. The new plate adherend just after removing

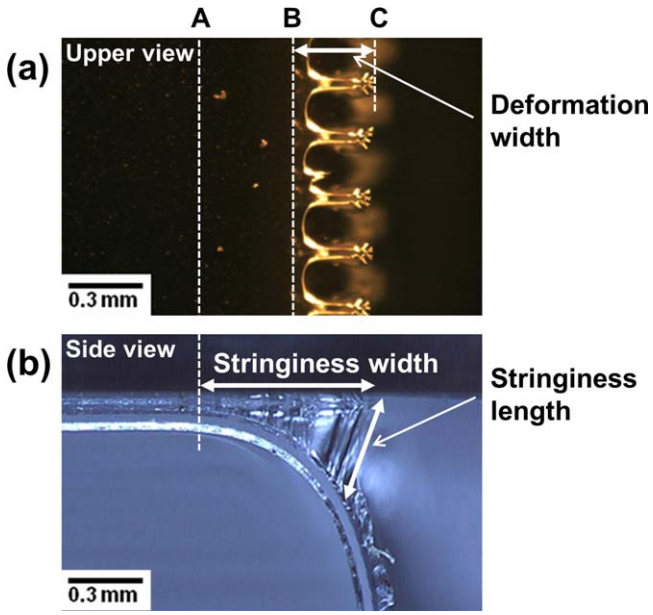

Figure 1. (a) Upper and (b) side views of stringiness during 90° peeling of crosslinked P(BA-AA) PSA with PMMA adherend under constant peel load of 2 N. The crosslinker content is 0.016 Eq. [Color figure can be viewed in the online issue, which is available at wileyonlinelibrary.com.]

a protection film was always used for stringiness observation.

Surface Roughness of Adherend

The surface roughness of the adherend was measured using a surface profiler (Alpha-Step IQ, KLA-Tencor, Milpitas, CA, USA). The measured range was 3 mm. The calculated average roughness (Ra), the 10-point average roughness (Rz), and the maximum height (Rmax) were measured. The average value of three measurements was shown.

Critical Surface Tension

The critical surface tension (γ_c) of the adherend was measured in accordance with the Zisman method.[14] The adherend surface was washed by 2-propanol and dried beforehand. The following five standard liquids having well-known critical surface tensions were used: polyethylene glycol (surface tension: 43.5 mN/m, number average molecular weight (M_n) of 400, viscosity of 7300 centistokes at 99°C), ethylene glycol (47.7 mN/m), diiodomethane (50.8 mN/m), glycerol (63.4 mN/m), and distilled water (72.8 mN/m). The contact angle was measured using a contact angle measuring device (Simage 02V, Excimer, Kanagawa, Japan) at 23–25°C. The quantity of the dropped standard liquid was

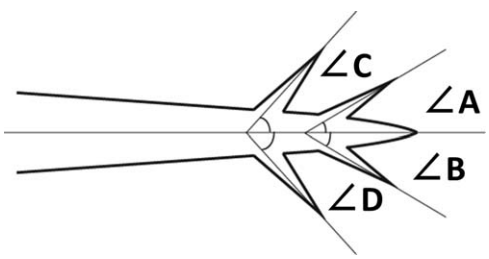

Figure 2. Measurement of angle of sub-branch.

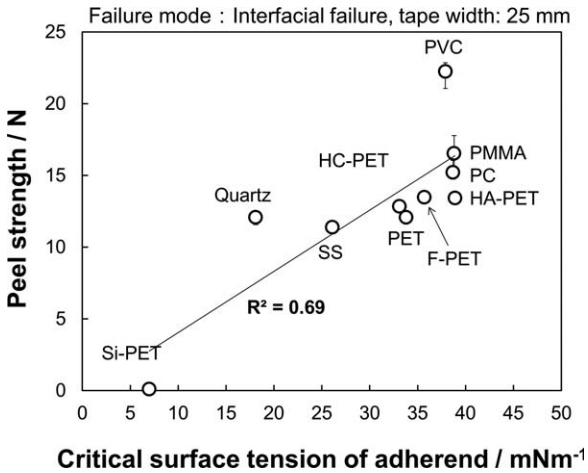

Figure 3. Effect of critical surface tension of adherend on 180° peel strength of crosslinked P(BA-AA) PSA. The crosslinker content is 0.016 Eq. The tape width is 25 mm.

1 μL (1×10^{-9} m^3) and the contact angle was measured 10 seconds after dropping.

RESULTS AND DISCUSSION

In our previous report,[10] the influence of the crosslinking degree of P(BA-AA) PSA on the stringiness shape was investigated. For this purpose, the crosslinker content was varied from 0 to 0.016 Eq. As Tse[15] and Yang[16] pointed out, the adhesion strength is shown by the multiplication of the interfacial adhesion at the adherend interface and the cohesive strength of the PSA. The cohesive strength of PSA increases with an increase in crosslinking degree, whereas the interfacial adhesion decreases. In this paper, in order to clearly observe the differences in interfacial adhesion with various adherends, the PSA that showed the lowest interfacial adhesion in this range was used (0.016 Eq.).

Peel Strength

The influence of adherend on the 180° peel strength is shown in Figure 3. All peeling was interfacial failure and independent of the adherend. The peel strength increased with an increase in the critical surface tension of adherend. The contribution ratios (R^2) are also shown in this Figure. The cohesive strength of a PSA is strongly affected by the peel rate because of a typical viscoelastic material. In this case, the PSA had sufficient cohesive strength because of a fast peel rate of 300 mm·min^{-1}. Therefore, the peel strength in Figure 3 is caused by the difference in the interfacial adhesion.

The peel strength with PVC was the highest. This seemed to be caused by the intermolecular interaction between AA unit in P(BA-AA) and PVC. About this point, we will be clarified by comparison the results of probe tack for crosslinked P(BA-AA) and crosslinked poly(2ethylhexyl acrylate-acrylic acid) random copolymer in the next report. There was no significant difference in the peel strength for PETs with various surface modifications. The peel strength with Si-PET adherend was the lowest. The critical surface tension used for the horizontal axis is an actual measured value, and that of SS was 26.1 mN/m. The

Table I. Surface Roughness of Adherend[a]

Adherend	Ra[b]	Rz[c]	Rmax[d]
Quartz	1	9	23
OPP	11	70	275
HA-PET	7	44	119
PET	22	142	549
HC-PET	6	25	71
F-PET	3	24	64
Si-PET	21	128	639
SS	13	68	133
PMMA	3	19	59
PC	3	15	31
PVC	9	43	79

[a] Unit: nm.
[b] Calculated average roughness.
[c] 10-point average roughness.
[d] Maximum height.

critical surface tension of metal must be larger than this because of the oxide layer that forms on the surface and the adsorbed organic materials as contaminants.

Stringiness Under Constant Peel Load

The surface roughness of adherends for stringiness observation measured using a surface profiler is shown in Table I. These values indicate that the surface of adherends is sufficiently smooth.

Figure 4 shows the digital microscope images of the upper views for the stringiness of crosslinked P(BA-AA) with various adherends under a constant peel load of 2 N. The measured peel rates were (a) 7.5, (b) 1.9, (c) 1.4, (d) 1.8, (e) 1.6, (f) 1.3, (g) 0.32, (h) 0.21, and (i) 0.18 mm·min^{-1}. The peeling mode was interfacial failure for all adherends. The typical sawtooth-shaped stringiness was observed independent of adherend, but the stringiness width was longer and clear sub-branches formed at the tips of the strings for PMMA (g), PC (h) and PVC (i). These adherends showed higher peel strength, as shown in Figure 3.

Figure 5 shows digital microscope images of the side views for the same samples as above. The stringiness length was also longer for PMMA (g), PC (h), and PVC (i).

The comparison of upper and side views of stringiness for PMMA adherend is shown in Figure 1. The stringiness was observed from point A in the side view [Figure 1(b)]. Deformation was never observed between points A and B in the upper view [Figure 1(a)]. This is because the deformation between points A and B is the elastic deformation, whereas the deformation between points B and C, observed as the sawtooth-shaped stringiness, is plastic deformation. The deformation width observed from the upper view and the stringiness width observed from the side view were measured and compared in Figure 6. The stringiness width was longer than the deformation width for all adherends. The ratio seems to be similar independent of the adherend. As SS adherend is not transparent, the deformation width could not be measured from the upper side.

The peel rate under constant peel load (2 N) for stringiness observation with various adherends was measured. The (logarithmic) peel rate under constant peel load and the peel strength measured in Figure 3 are plotted in Figure 7. The peel rate decreased with the increase in peel strength. It was found

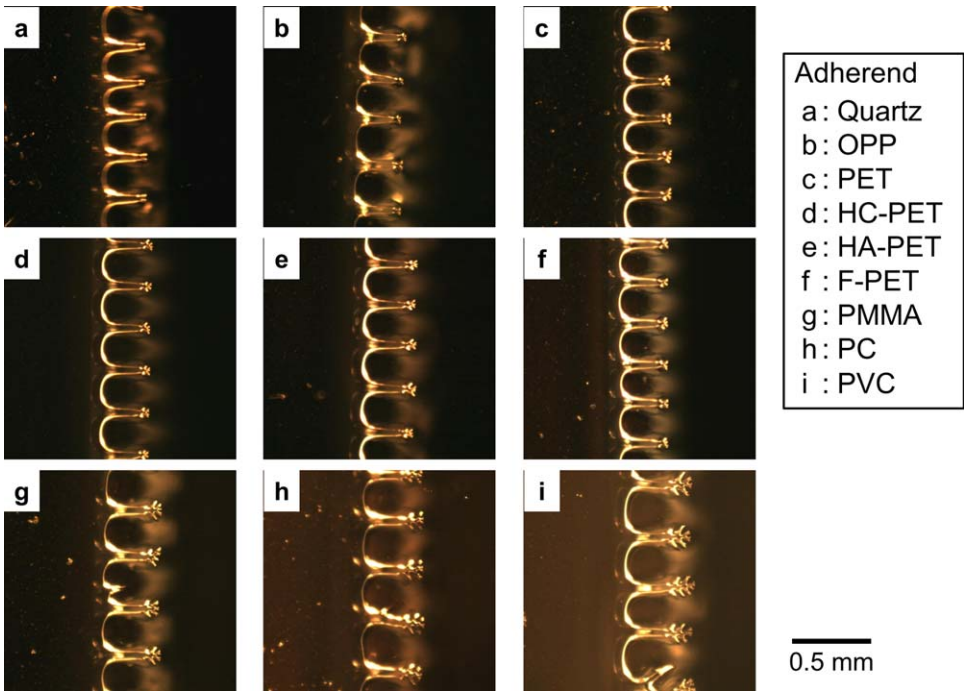

Figure 4. Upper views of stringiness during 90° peeling of crosslinked P(BA-AA) PSA with various adherend under constant peel load of 2 N. The crosslinker content is 0.016 Eq. [Color figure can be viewed in the online issue, which is available at wileyonlinelibrary.com.]

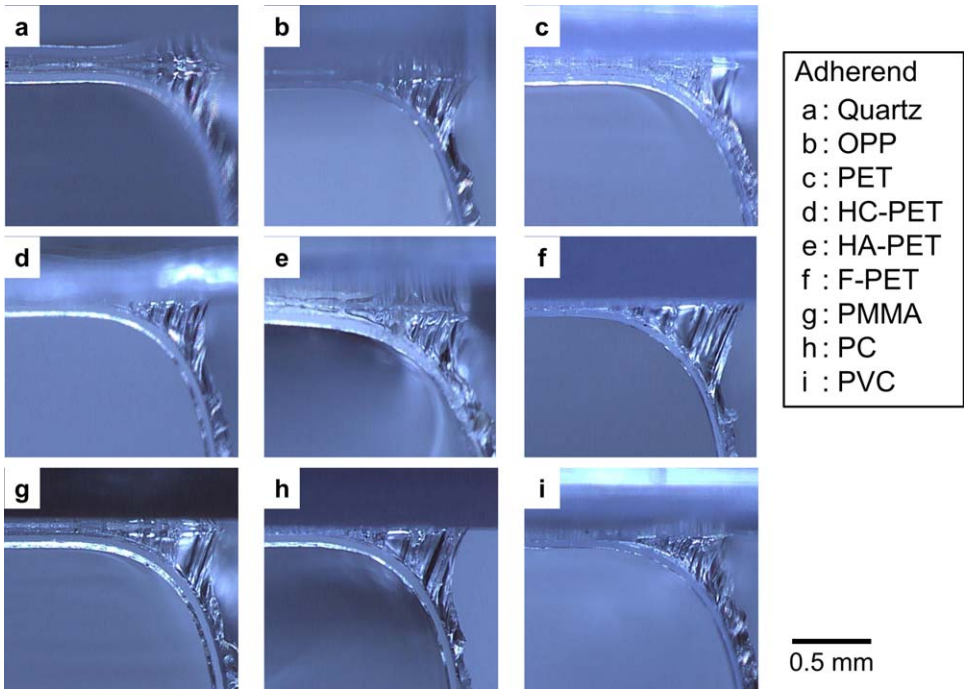

Figure 5. Side views of stringiness during 90° peeling of crosslinked P(BA-AA) PSA with various adherend under constant peel load of 2 N. The crosslinker content is 0.016 Eq. [Color figure can be viewed in the online issue, which is available at wileyonlinelibrary.com.]

that the peel rate under constant peel load has good correlation with the peel strength.

The stringiness width, the stringiness length, the deformation width, and the angle of sub-branches are plotted against the (logarithmic) peel rate under constant peel load and are shown in Figure 8. All of these values showed linear relationships with the peel rate. These showed a good correlation with the peel rate under constant peel load, indicating that they also have good relationship with the peel strength.

Stringiness Under Constant Peel Rate

The previous section presented the stringiness under constant peel load; however, each peel rate was different. The PSA is a typical viscoelastic material, such that the elastic modulus is strongly dependent on the peel rate. The stringiness under constant peel rate was investigated. The comparison of the influence of the interfacial adhesion on the stringiness is possible only under the constant peel rate condition.

Preliminary tests were conducted in which various loads were used and the peel rate for each was measured. The relationship between the (logarithmic) peel rate and the applied load is shown in Figure 9. The PSA with PVC adherend required the largest load and that with PC was the second largest. From these results, the ideal peel rate was determined to be 1.2 $mm \cdot min^{-1}$ (0.08, logarithmic; dashed line in Figure 9) for the constant peel rate test, and the peel load that shows the peel rate closest to 1.2 $mm \cdot min^{-1}$ was used.

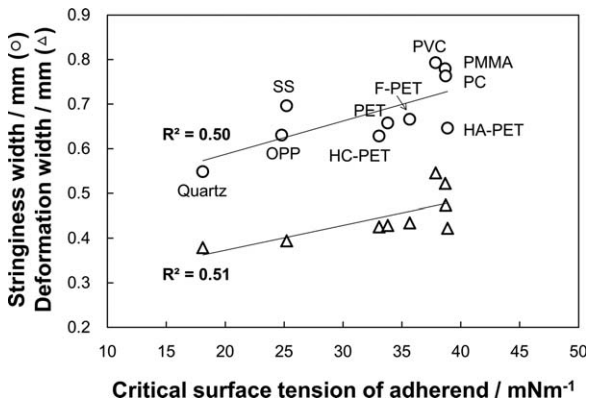

Figure 6. Influence of critical surface tension of adherend on stringiness width (○) and deformation width (△) during 90° peeling of crosslinked P(BA-AA) PSA under constant peel load of 2 N. The crosslinker content is 0.016 Eq.

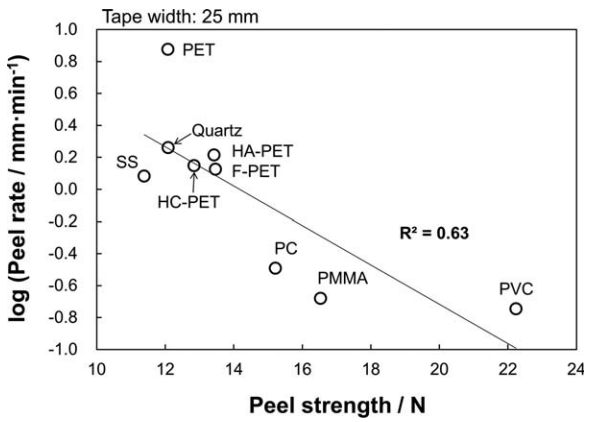

Figure 7. Relationship between peel rate under constant peel load of 2 N and peel strength of crosslinked P(BA-AA) PSA. The crosslinker content is 0.016 Eq. The tape width is 25 mm.

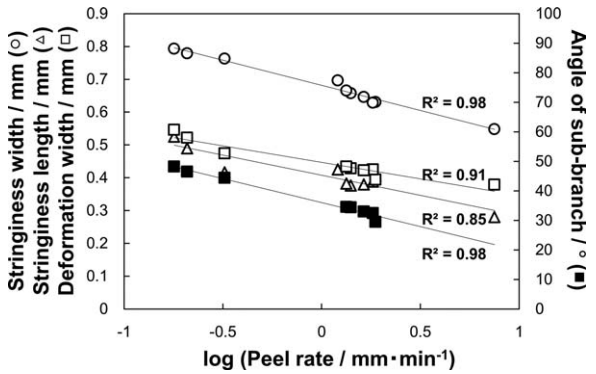

Figure 8. Influence of peel rate on stringiness width (○), stringiness length (△), deformation width (□) and angle of sub-branch (■) during 90° peeling of crosslinked P(BA-AA) PSA under constant peel load of 2 N. The crosslinker content is 0.016 Eq.

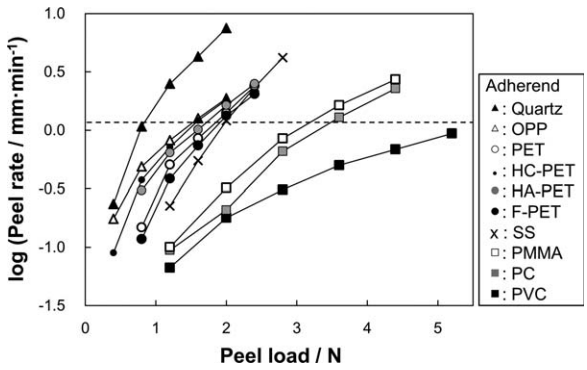

Figure 9. Influence of peel load on peel rate during 90° peeling of crosslinked P(BA-AA) PSA with various adherend. The crosslinker content is 0.016 Eq. The dashed line indicates the peel rate of 1.2 mm·min^{-1} (0.08, logarithmic).

Figure 10 shows the digital microscope images for the upper views of stringiness of crosslinked P(BA-AA) under a constant peel rate of ca. 1.2 mm·min^{-1}. The actual peel rates were (a) 1.1, (b) 1.3, (c) 0.9, (d) 1.0, (e) 1.2, (f) 1.3, (g) 0.85, (h) 1.3, and (i) 0.94 mm·min^{-1}. The peel loads required for these peel rates were (a) 0.8, (b) 1.6, (c) 1.6, (d) 1.6, (e) 1.6, (f) 2.0, (g) 2.8, (h) 3.6, and (i) 5.2 N. The peel mode was interfacial failure except for PVC adherend where it was cohesive failure. The typical sawtooth-shaped stringiness was observed independent of adherend. Frames formed at the front end of the strings for PVC adherend. The stringiness width was shorter for quartz (a) and OPP (b) adherends and longer for PMMA (g), PC (h), and PVC (i). PET (c) and some surface modified PETs (d–f) had intermediate widths. Small sub-branches were observed at the tip of the strings for PET (c) and some surface modified PETs (d–f). The sub-branches became more significant for PMMA (g), PC (h), and PVC (i).

Figure 11 shows the digital microscope images for side views of these same samples under a constant peel rate. The stringiness width and length showed the same tendency as the above-mentioned deformation width.

All observed stringiness was the typical sawtooth-shaped type, but the sawtooth-shaped type with front frame was also observed for PVC adherend under a constant peel rate, as

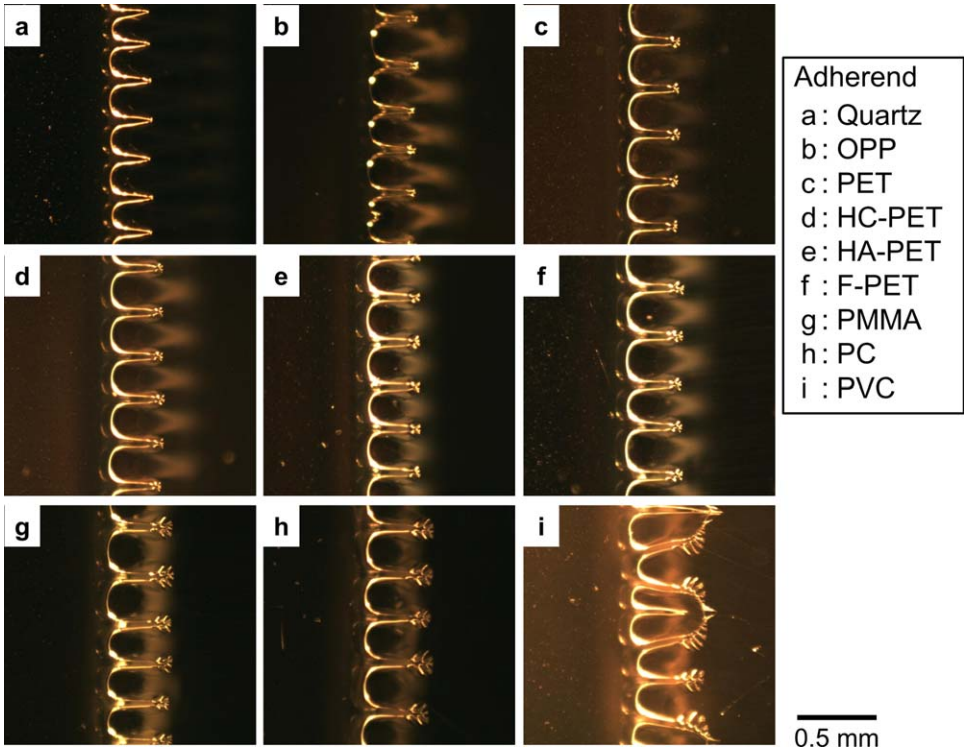

Figure 10. Upper views of stringiness during 90° peeling of crosslinked P(BA-AA) PSA with various adherend under constant peel rate of ca. 1.2 mm·min^{-1}. The crosslinker content is 0.016 Eq. [Color figure can be viewed in the online issue, which is available at wileyonlinelibrary.com.]

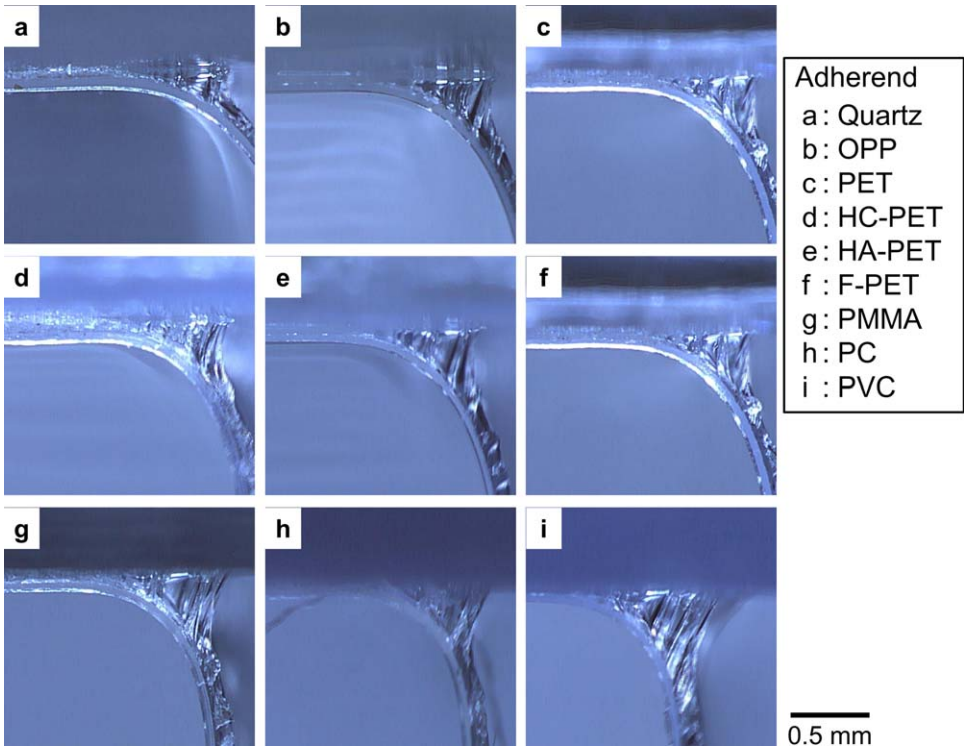

Figure 11. Side views of stringiness during 90° peeling of crosslinked P(BA-AA) PSA with various adherend under constant peel rate of ca. 1.2 mm·min^{-1}. The crosslinker content is 0.016 Eq. [Color figure can be viewed in the online issue, which is available at wileyonlinelibrary.com.]

schematically shown in Figure 12. The reason why the sawtooth-shaped stringiness formed is thought to be due to the negative pressure that arises in the tip part of the extended PSA layer. As a result, air invades the PSA layer equally from the tip part, which then pushes the PSA layer at equal intervals from the peeling front.

In the case of PVC adherend, the interfacial adhesion is highest. This results in large internal deformation of the PSA layer. Internal deformation occurs preferentially over peeling and the front frame forms as a result. Therefore, the peel mode was cohesive failure only for PVC adherend. That is, the shape of stringiness observed in this study is strongly dependent on the interfacial adhesion.

Clear sub-branches were observed for PMMA (g), PC (h), and PVC (i) adherends as shown in Figure 10. These adherends showed higher interfacial adhesion. In the case of higher interfacial adhesion, a similar phenomenon for the sawtooth-shaped stringiness formation also occurred at the tip of the strings, forming sub-branches. The depiction of the sub-branches is omitted in Figure 12.

The relationship between constant peel rate and the peel strength is shown in Figure 13. There was good correlation.

The stringiness width, the stringiness length, and the angle of sub-branches were measured from Figures 10 and 11 and plotted against the peel load for constant peel rate as shown in Figure 14. The R^2 values are also shown in this Figure. All of these values showed good correlation with the peel load for constant peel rate.

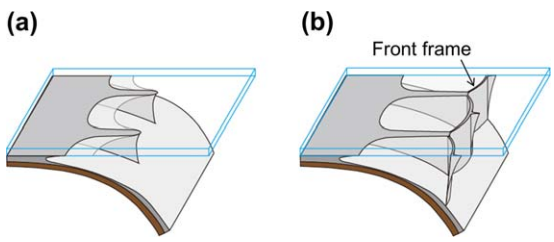

Figure 12. Schematic views of (a) typical type and (b) front frame type of sawtooth-shaped stringiness. [Color figure can be viewed in the online issue, which is available at wileyonlinelibrary.com.]

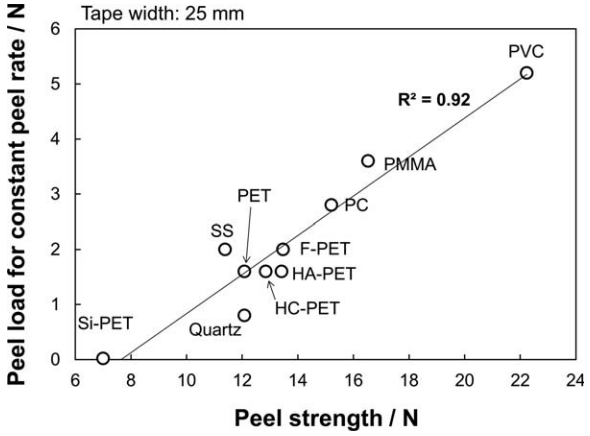

Figure 13. Relationship between peel load for constant peel rate of ca. 1.2 mm·min^{-1} and peel strength of crosslinked P(BA-AA) PSA. The crosslinker content is 0.016 Eq. The tape width is 25 mm.

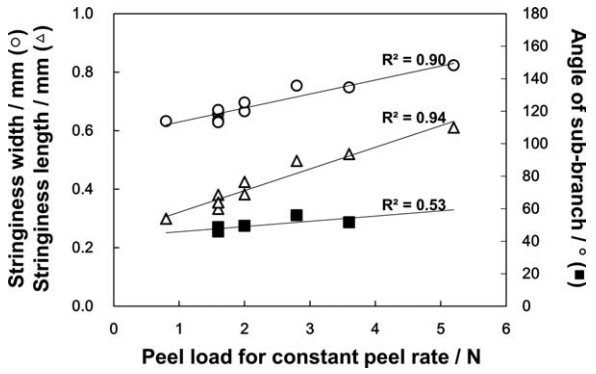

Figure 14. Influence of peel load on stringiness width (○), stringiness length (△) and angle of sub-branch (■) during 90° peeling of crosslinked P(BA-AA) PSA under constant peel rate of ca. 1.2 mm·min^{-1}. The crosslinker content is 0.016 Eq.

Generated Inner Stress in Fibril

The generated inner stress in the fibril string was estimated. This estimation was performed by assuming that the tip of stringiness is fibril-like. This should relate to the peel strength. The stringiness length (L) and width (W) were used for this estimation. The time required for peeling to progress over distance W is defined as the deformation time (t_d). The peel rate (r_p) is shown as

$$r_p = \frac{W}{t_d} \quad (1)$$

It was assumed that the t_d is equal to the time that the fibril length extends from 0 to L. The deformation rate (r_d), i.e., the rate for the fibril length to extend from 0 to L is shown by

$$r_d = \frac{L}{t_d} \quad (2)$$

In this article, the thickness of the PSA layer was approximately 50 μm and the constant peel rate test was performed at ca. 1.2 mm·min^{-1}, thus the r_d was calculated as 0.2 s^{-1}.

The tensile test of PSA was performed at 100 mm·min^{-1} with a chuck distance of 10 mm, thus the r_d was equal to the r_d of 0.17 s^{-1}. This is close to the r_d of the abovementioned constant peel rate test, 0.2 s^{-1}. The recorded stress–strain curve is shown in Figure 15. The stringiness length shown in Figure 14 was converted to the strain rate using the measured average thickness of the PSA layer, 55 μm. The calculated strain rates for various adherends are shown in Table II. The maximum strain of the stress–strain curve was 1098%. The strain rate for the PVC adherend was 1135%, which was larger than the actual maximum strain. Therefore, the stress at the maximum strain could not be calculated for the PVC adherend. This is the reason why the peel test for stringiness observation with PVC adherend showed cohesive failure as mentioned above. The stress at each strain rate was obtained by assigning the strain rate for various adherends shown in Table II into the stress–strain curve as shown in Figure 15. The obtained stress values are also shown in Table II. These obtained stress values are related to the maximum inner stress generated in the stringiness.

Table II. Calculated Strain and Stress of Crosslinked P(BA-AA) PSA

Adherend	Strain[a] (%)	Stress[b] (MPa)
Quartz	587	0.150
OPP	624	0.163
HA-PET	663	0.177
PET	672	0.180
HC-PET	720	0.194
F-PET	725	0.195
SS	804	0.226
PMMA	950	0.281
PC	976	0.294
PVC	1135	-

[a] Calculated from the stringiness length.
[b] Calculated from the stress–strain curve of PSA.

The relationship between the generated inner stress and the peel load for the constant peel rate is shown in Figure 16, showing linear relationships for all of them. In other words, an adherend with higher interfacial adhesion requires a larger inner stress for peeling. It is thought that the generated inner stress and the peel strength have good correlation. That is, the peel strength

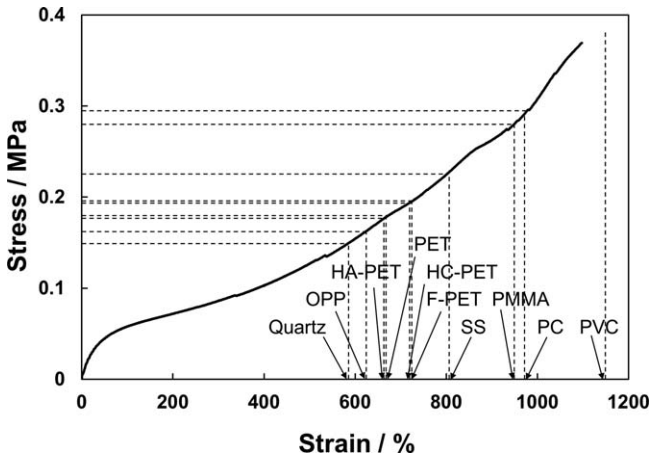

Figure 15. Stress–strain curve of crosslinked P(BA-AA) PSA. The crosslinker content is 0.016 Eq.

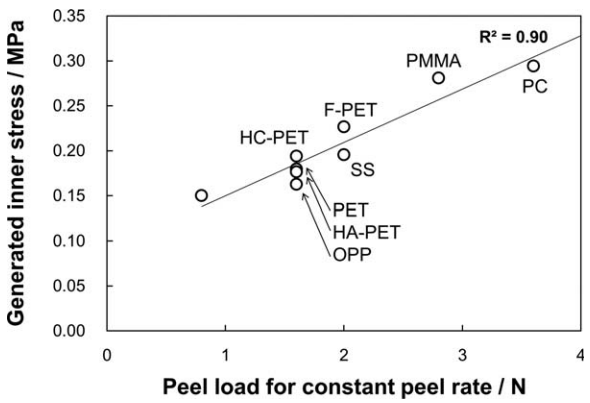

Figure 16. Relationship between estimated inner stress and peel load for constant peel rate of ca. 1.2 mm·min^{-1} of crosslinked P(BA-AA) PSA. The crosslinker content is 0.016 Eq.

can be estimated from the stress–strain curve of PSA and the stringiness length.

CONCLUSIONS

In order to clarify the influence of interfacial adhesion on the stringiness behavior, the stringiness of crosslinked P(BA-AA) with various adherends during 90° peeling was observed under both constant peel load and constant peel rate. The crosslinker content was 0.016 Eq. The following results were obtained:

i. The 180° peel strength was higher in the order of PVC >> PMMA ≈ PC > other adherends.
ii. All observed stringiness was sawtooth-shaped, but the stringiness width and length were longer for PVC, PMMA, and PC adherends. The sub-branches formed at the tips of the strings increased for these adherends. Frames formed at the front end of the strings in the case of PVC adherend. Sufficient interfacial adhesion generates large internal deformation of the PSA layer. Internal deformation occurred preferentially over peeling as a result of front frame formation.
iii. The stringiness length and the peel load required for the constant peel rate have good correlation with the peel strength.
iv. The estimation of generated inner stress in the stringiness fibrils was possible by analysis using the stringiness length for various adherends and the stress–strain curve of pure PSA.

ACKNOWLEDGMENTS

The authors are grateful to Toagosei (Tokyo, Japan) for the polyacrylic polymer preparation and to Mitsubishi Gas Chemical Company (Tokyo, Japan) for donation of the crosslinker.

REFERENCES

1. Kaelble, D. H. *Trans. Soc. Rheol.* **1965**, *9*, 135.
2. Urahama, Y. *J Adhesion* **1989**, *31*, 47.
3. Hino, K.; Hashimoto, H. *J. Appl. Polym. Sci.* **1985**, *30*, 3369.
4. Zosel, A. *J. Adhes.* **1989**, *30*, 135.
5. Yamazaki, Y.; Toda, A. *J. Phys. Soc. Jpn.* **2002**, *71*, 1618.
6. Yamazaki, Y.; Toda, A. *J. Phys. Soc. Jpn.* **2004**, *73*, 2342.
7. Miyagi, Z.; Koike, M.; Urahama, Y.; Yamamoto, K. *Int. J. Adhes. Adhes.* **1994**, *14*, 39.
8. Williams, J. A.; Kauzlarich, J. *J. Int. J. Adhes. Adhes.* **2008**, *28*, 192.
9. Vilmin, T.; Ziebert, F.; Raphaël, E. *Langmuir* **2010**, *26*, 3257.
10. Ito, K.; Shitajima, K.; Karyu, N.; Fujii, S.; Nakamura, Y.; Urahama, Y. *J. Appl. Polym. Sci.* **2014**, *131*, 5550.
11. Nakamura, Y.; Sakai, Y.; Adachi, M.; Fujii, S.; Sasaki, M.; Urahama, Y. *J. Adhes. Sci. Technol.* **2008**, *22*, 1313.
12. Nakamura, Y.; Imamura, K.; Yamamura, K.; Fujii, S.; Urahama, Y. *J. Adhes. Sci. Technol.* **2013**, *27*, 1951.
13. Nakamura, Y.; Adachi, M., Ito, K.; Kato, Y.; Fujii, S.; Sasaki, M.; Urahama, Y.; Sakurai, S. *J. Appl. Polym. Sci.* **2011**, *120*, 2251.
14. Zisman, W. A. *Ind. Eng. Chem.* **1963**, *55*, 18.
15. Tse, M. F. *J. Adhes. Sci. Technol.* **1989**, *3*, 551.
16. Yang, H. W. H. *J. Appl. Polym. Sci.* **1989**, *55*, 645.